High Curvature Concave–Convex Microlens

Jun-Jie Xu, Wen-Gang Yao, Zhen-Nan Tian, Lei Wang, Kai-Min Guan, Ying Xu, Qi-Dai Chen, Ji-An Duan, and Hong-Bo Sun, *Member, IEEE*

***Abstract*— We report in this letter a concave–convex microlens (CCML) consisting of two different high curvature surfaces. Compared with the conventional plano-convex microlenses, the CCML not only allows for more design freedom, but also offers significantly improved optical performance, particularly minimization of aberration, as is critical when the size of optical components is small. Experimentally, focusing capability at different wavelengths was demonstrated, and the axial chromatic aberration was found significantly reduced to ∼4.6% of the focal length shift under wavelength 450–660 nm.**

***Index Terms*— Concave-convex microlens, femtosecond laser direct writing, design freedom, high curvature.**

I. Introduction

In THE past few decades, the microlens and its array have been widely applied in micro-optical system as a new promising generation optical elements. Especially in beam shaping [1], artificial compound eyes [2], photocopying [3], and high speed parallel optical switching networks [4], microlenses are playing an irreplaceable role due to small size, light weight, and high optical performance. A series of fabrication technologies were proposed to prepare microlens including soft lithography [5], gray scale lithography [6], thermal reflow [7], and solvent evaporation self-organization [8]. Microlenses of diameters ranging from millimeters to micrometers were readily produced. The lenses attained so far are all of plano-convex or plano-concave architecture due to the limitation of prototyping capability of above technologies. The geometry is not only a waste of one surface design freedom but also introduces more aberrations [9] when the lens possesses a high curvature surface. D. Wu et al. designed an aspheric lens to reduce optical aberrations with a low curvature surface [10]. Surface curvature is important for an optical lens, especially those in imaging and near-field recording systems [11]. The surface of microlens is connected to object space and determines the numerical aperture, which closely associated with aberration and resolution of a lens. For conventional microlens whose second surface is a plane, the ability of light refraction can only be adjusted by regulating the curvature of the first surface. The great difference of the optical path between central region and edges brings aberrations [9]. When the first surface was a high curvature, the aberration would be reduced by changing the second surface to reduce the difference of the optical path between central region and edges.

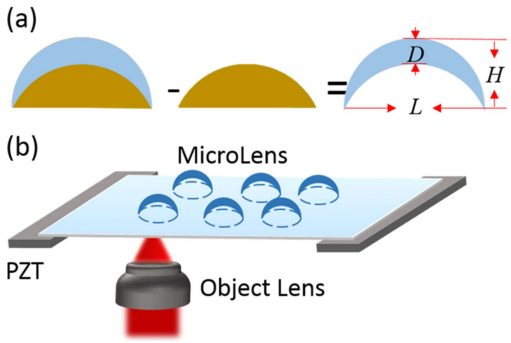

Fig. 1. (a) Schematic of the design of the concave-convex lens. The lens' thickness is D. (b) Schematic diagram of the preparation of micro-lens by FsLDW.

A. Žukauskas et al. fabricated micro-optical elements [12], especially a fiber tip microoptical component consisted of an aspherical and a conical lens [13] to lower the demand on alignment tolerance via mode field expansion by direct laser writing of photopolymers [14], [15]. Here, we propose the concave-convex microlens (CCML) concept for the first time, and experimentally accomplished the fabrication by femtosecond laser direct writing (FsLDW) induced two-photon polymerization [16], [17], a technology known for its unique high-precision [18] three-dimensional (3D) prototyping capability [19]. The curvature and thickness of the CCML were precisely controlled, as guarantees the desired high performance of the microlenses, which were then experimentally confirmed.

II. Experiments

The cross section schematic diagram of the spherical concave-convex microlens (CCML) is shown in Fig. 1(a), where D is the thickness of the lens. It is obtained by subtracting a small plano-convex lens (the yellow part in Fig. 1(a)) from the common plano-convex lens. The CCML was written by two-photon polymerization of the negative photoresist

Manuscript received June 9, 2015; revised July 25, 2015; accepted August 16, 2015. Date of publication September 7, 2015; date of current version October 2, 2015. This work was supported in part by the National Basic Research Program of China under Grant 2011CB013005 and Grant 2014CB921302, and in part by National Natural Science Foundation of China under Grant 61137001, Grant 61127010, Grant 91423102, and Grant 91323301.

J.-J. Xu, W.-G. Yao, Z.-N. Tian, L. Wang, K.-M. Guan, Y. Xu, Q.-D. Chen, and H.-B. Sun are with the State Key Laboratory on Integrated Optoelectronics, College of Electronic Science and Engineering, Jilin University, Changchun 130012, China (e-mail: chenqd@jlu.edu.cn; hbsun@jlu.edu.cn).

J.-A. Duan is with the State Key Laboratory of High Performance Complex Manufacturing, Central South University, Changsha 410083, China.

Color versions of one or more of the figures in this letter are available online at http://ieeexplore.ieee.org.

Digital Object Identifier 10.1109/LPT.2015.2470195

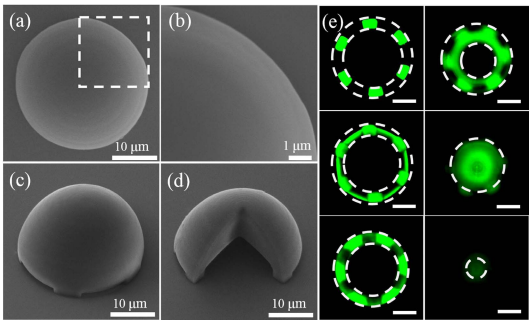

Fig. 2. (a) Top-view scanning electron microscopy (SEM) image of a concave-convex microlens (CCML). (b) Enlarged view of the marked area in (a), (c) and (d) 45° tiled-view SEM image of the CCML and three quarters of the CCML. (e) Laser scanning confocal microscopy (LSCM) image of the CCML in different Z axis position. Scale bar: 10μm.

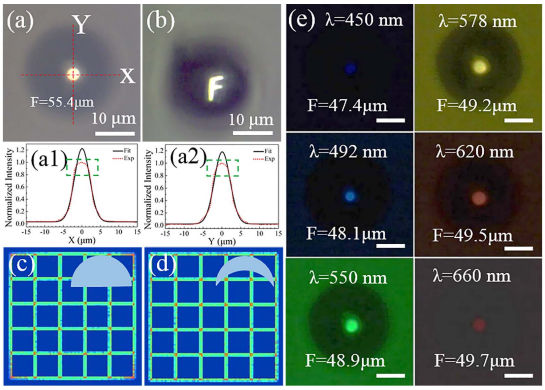

Fig. 3. (a) Focal spot image of the lens at the focal plane under illumination with quasi parallel light from a halogen lamp. The focal length (F) measured is ~55μm. (a1) and (a2): normalized light intensity distribution and Gauss fitting curve along the dotted line across the center of (a) in the x-direction and y-direction. (b) Optical microscope characterization of the imaging of the lens. (c) and (d) Imaging simulation of object (5×5 grids) in the distance of twice lens focal length via plano-convex lens and CCML by ZEMAX, respectively. (e) Focal length (F) of the lens for monochromatic light with different wavelengths in air. Scale bar: 10μm.

resin SU-8 (2025, MicroChem). With 120 fs pulse width and 82MHz repetition rate and 800nm central wavelength (from Tsunami, Spectra-Physics), the laser was tightly focused through the substrate by a high numerical aperture (NA = 1.4) oil immersion objective lens (100×), so as to induce polymerization in the central area of the focus spot. Then, the focus spot was moved along the optical axis by the peizo stage, and along the horizontal plane by steering a two-galvano mirror set. The photoresist samples were prepared by spin-coating SU-8 films on a cover glass that was ultrasonic cleaned with acetone and absolute ethanol for 30 minutes. Then the photoresist was soft-baked for 30 minutes at 95 °C to evaporate the solvent. Thick films were obtained. The average laser power of polymerization was 8mW before the objective towards the laser, scanning step length was 100 nm in three dimensions and exposure duration of each voxel was 500 μs. Laser focus spot was scanned point by point from the bottom slice to the upside slice according to the computer preprogrammed patterns. The concentration of acid was generated following the distribution of the square of light intensity [20]. After fabricated, the patterned sample was post-baked for 15 minutes at a temperature of 95 °C, so as to convert the potential patterns into cross-linked solid skeleton by a cationic photo amplification. Finally, the sample was rinsed in the developer for 20 minutes to remove the unpolymerized photoresist. The designed device structure was remained on chip [Fig. 1(b)].

III. Results and Discussion

As is known to all, the structure 3D shape and surface roughness [10] of a lens play vital roles on its imaging. Here, we fabricated the special 3D shaped concave-convex microlens (CCML) with high surface quality, taking the advantages of high machining accuracy and shape designability of FsLDW. In the optimization of machining parameters mentioned above, we prepared the desired microlens. In Fig. 2, the CCML was investigated and characterized by scanning electron microscopy (SEM, JSM-7500F, JEOL) and laser scanning confocal microscope (LSCM, FV1000). From the top-view SEM image of the CCML [Fig. 2(a)], we can find that the diameter (L) of the CCML is 30μm. Due to the self-smoothing effect caused by local surface tension during the rinsing step [10], high quality curved surface was attained [Fig. 2(b)]. In this work, to gain the optimal self-smoothing behavior, a mall enough step scanning and high homogeneity of the sizes of the voxel were needed. As the uniformity of voxel sizes is related to the square of photopolymerization rate which depends on laser light intensity, slight variations of laser pulse energy may produce uneven surface. Therefore, the fluctuation of pulse energy should be fixed at lower than 0.5%. In order to achieve this demand, we keep the indoor temperature around the laser within (23±0.2)°C and assemble an output feedback system in the experiment. Here, the height (H) of CCML (not include height of pillars) was designed to be 12 μm. Images shown in Fig. 2(c) and Fig. 2(d) are the 45°-tiled SEM image of the complete CCML and three quarters of the CCML, respectively. Pillars were designed to let the unexposed resist out when developing. The empty interior of the CCML is shown in Fig. 2(d). In order to quantitatively examine the interior profile, a LSCM was used. We previous prepared the same CCML via two-photon polymerization of SU-8 doped with Rhodamine B by FsLDW. Through LSCM characterization of the CCML, we have the cross-sectional fluorescent images along the different position of Z axis position from the bottom slice to the upside slice, shown as Fig. 2(e). From a series of LSCM images, we recognize that cross sections of the internal and the external outlines (the dotted circles) are circular. As the LSCM imaging position changed gradually, these features are consistent with the outline of the lens. There is no impurity in the interior of the CCML, which shows unexposed resist of the CCML's interior had all been developed. These results demonstrate that digital microlens has been faithfully converted to the desired device structure by femtosecond laser-induced two-photon polymerization.

Because of the fine morphology, the CCML exhibited excellent optical performances [Fig. 3]. They were characterized with an optical microscopic setup. A bright

focal spot was observed [Fig. 3(a)]. The normalized intensity distribution (the red dotted line) and the Gauss fitting curve (the black line) along the red line across the center of the CCML in the x-direction and the y-direction of Fig. 3(a) were shown in Fig. 3(a1) and Fig. 3(a2). The intensity distribution was saturated in the peak position marked with green dotted line, so we have fitted the effective data (non-peak). The full width at half maximum (FWHM) of the fitting curve was $\sim 5\mu$m. While Y. L. Sun et al. reported that a protein spherical microlens (a radius of 20 μm and a height of 5 μm) exhibited an FWHM of ~ 15 μm [21]. Imaging ability of the lens was found to be very clear and bright, as shown in Fig. 3(b). Focal length of the CCML is calculated according to the thick lens focus formula:

$$f = \frac{n_{SU-8} n_0 R_1 R_2}{(n_{SU-8} - n_0)\left[(n_{SU-8} - n_0) - n_{SU-8}(R_1 - R_2)\right]} \tag{1}$$

$$x_H = \frac{-D n_0 R_2}{D(n_{SU-8} - n_0) - n_{SU-8}(R_1 - R_2)} \tag{2}$$

where x_H is the main point position of the thick lens, R_1 and R_2 represent the internal and the external curvature radii of the concave and convex lens, D is the lens' thickness. n_{SU-8} and n_0 are refractive index of photoresist SU-8 and environment around the lens, respectively. Herein, we define $F(F = f + x_H)$ as the actual focal length, which is used to represent the distance from the focal spot to the surface of the microlens. It could be detected when the object lens was moved from far to near. Shown in Fig. 3, Given $D = 8$ μm, $H = 12$ μm, and $L = 30$ μm, we gain $R_1 = -30.125$ μm and $R_2 = -15.375$ μm by the Pythagorean Theorem. We had $F = 49.1$ μm under white light illumination when $n_{SU-8} = 1.5858$, agreed with the measured value of 55.4 μm. The CCML we prepared would be useful for common optical design, such as the achromatization of lens systems. We measured the focal lengths of the CCML for monochromatic light with different wavelengths in air shown in Fig. 3(e). The maximum shift of focal length was $\sim 4.6\%$, which is defined as $(F_{\max} - F_{\min})/F_{\max}$, where $F_{\max}$ and $F_{\min}$ denote the maximum and the minimum of the focal length in Fig. 3(e). The result showed that the axial chromatic aberration was significantly reduced, which is an important parameter in multi-wavelength optical system. Moreover, we used the ray tracing method to simulate and analyze the geometry imaging capability of lens via ZEMAX, shown in Fig. 3 (c) and Fig. 3 (d). To better characterize the imaging effect of different location of the object, the imaging object (the size of 10μm) was composed of 5×5 grids. Different positions of the grid array represent different field of view. Relative to the side, the intersection point (the red dot) of grids could more clearly show fuzzy of imaging. The red color shows that the side of the object image more blur in the corner of Fig. 3(c) than in the corner of Fig. 3(d). It shows that CCML has a better ability of balance aberration than plano-convex lens with the same surface curvature, especially at a larger field of view as shown in four corners of imaging.

In addition to these optical properties above, CCML also exhibited more interesting adjustable focus feature. As shown in Fig. 4(a), the black line represents the theory curve of the focal length of the lens ($D = 8$ μm, $H = 12$ μm, and $L = 30$ μm) versus refractive index of the environment around the lens, according to focus formula mentioned above. Because the interior of the CCML is empty, the refractive index on both sides of the CCML is same. The red dot represents the measured value in four different environments, Air, H_2O, C_2H_5OH and $(CH_2OH)_2$, respectively. We used droplets to test the focus of the lens in liquid environment. The insets are focal spot images, shown in Fig. 4(a). We can find out that trend of the focal length of experiment versus refractive index is consistent with theory. The deviation of the focus of experiment and theory maybe caused by the shape of the droplet.

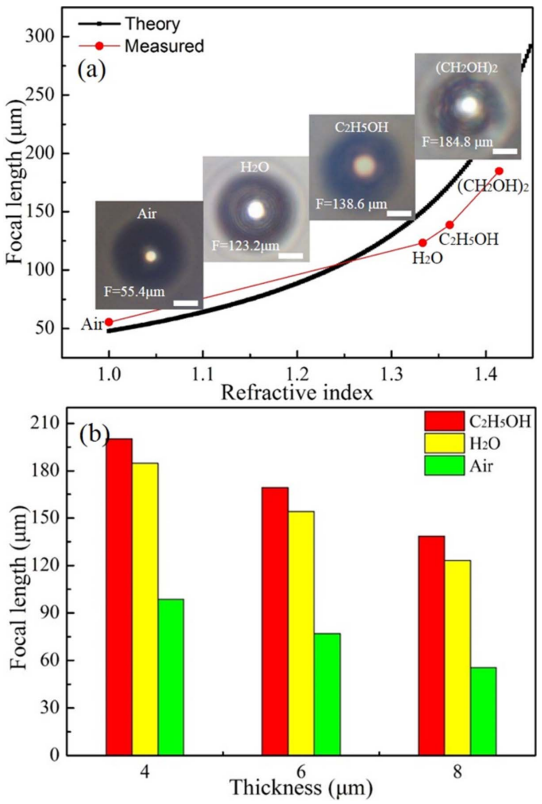

Fig. 4. (a) Focal length of the lens versus refractive index. The measured value (the red dot) and the theory profile (the black line). The insets are focal spot images of the lens under the refractive index in the different environment. Scale bar: 10μm. (b) Focal length of the lens versus thickness of the lens in different environment such as C_2H_5OH, H_2O and Air.

The 3D shape (mainly the thickness here, D) is another main factor determining the tunable focus property of CCML ($H = 12$ μm, and $L = 30$ μm). The measured focal length decreased with the thickness of the CCML increasing from 4 to 8 μm, in Air, H_2O and C_2H_5OH three different environments, respectively [Fig. 4(b)]. While the thickness of CCML was fixed at the certain value, the focal length increased with increasing of environment refractive index.

IV. Conclusion

In summary, a high curvature concave-convex microlens (CCML) was fabricated by a femtosecond laser induced two-photon polymerization technology. Compared to conventional plano-convex microlenses, the CCML not

only allows for more design freedom, but also offers significantly improved optical performance, such as imaging quality, capability of focusing and balancing aberration. The CCML would have great potential applications such as beam shaping [22] and integrated optical systems. In addition, the focal length of CCML will change along with the ambient refractive index. Using this tunable focus feature, CCML will be expected to be applied in microfluidic channel [23]. Moreover, due to CCML's hollow shape, it also may be applied to a miniature reaction chamber.

REFERENCES

[1] Z.-N. Tian *et al.*, "Beam shaping of edge-emitting diode lasers using a single double-axial hyperboloidal micro-lens," *Opt. Lett.*, vol. 38, no. 24, pp. 5414–5417, Dec. 2013.

[2] D. Wu *et al.*, "Bioinspired fabrication of high-quality 3D artificial compound eyes by voxel-modulation femtosecond laser writing for distortion-free wide-field-of-view imaging," *Adv. Opt. Mater.*, vol. 2, no. 8, pp. 751–758, Aug. 2014.

[3] Y.-P. Huang, H.-P. D. Shieh, and S.-T. Wu, "Applications of multidirectional asymmetrical microlens-array light-control films on reflective liquid-crystal displays for image quality enhancement," *Appl. Opt.*, vol. 43, no. 18, pp. 3656–3663, Jun. 2004.

[4] L. Erdmann and K. J. Gabriel, "High-resolution digital integral photography by use of a scanning microlens array," *Appl. Opt.*, vol. 40, no. 31, pp. 5592–5599, Nov. 2001.

[5] M. V. Kunnavakkam *et al.*, "Low-cost, low-loss microlens arrays fabricated by soft-lithography replication process," *Appl. Phys. Lett.*, vol. 82, pp. 1152–1154, Oct. 2003.

[6] Q. Peng, Y. Guo, S. Liu, and Z. Cui, "Real-time gray-scale photolithography for fabrication of continuous microstructure," *Opt. Lett.*, vol. 27, no. 19, pp. 1720–1722, Oct. 2002.

[7] H. Yang, C.-K. Chao, M.-K. Wei, and C.-P. Lin, "High fill-factor microlens array mold insert fabrication using a thermal reflow process," *J. Micromech. Microeng.*, vol. 14, no. 8, pp. 1197–1204, Aug. 2004.

[8] J. Y. Lee *et al.*, "Near-field focusing and magnification through self-assembled nanoscale spherical lenses," *Nature*, vol. 460, pp. 498–501, Jul. 2009.

[9] M. Born and E. Wolf, *Principles of Optics*, 7th ed. Cambridge, U.K.: Cambridge Univ. Press, 1999, p. 211.

[10] D. Wu *et al.*, "100% fill-factor aspheric microlens arrays (AMLA) with sub-20-nm precision," *IEEE Photon. Technol. Lett.*, vol. 21, no. 20, pp. 1535–1537, Oct. 15, 2009.

[11] L. Li, W. Guo, Y. Yan, S. Lee, and T. Wang, "Label-free super-resolution imaging of adenoviruses by submerged microsphere optical nanoscopy," *Light, Sci. Appl.*, vol. 2, p. e104, Sep. 2013.

[12] A. Žukauskas, M. Malinauskas, and E. Brasselet, "Monolithic generators of pseudo-nondiffracting optical vortex beams at the microscale," *Appl. Phys. Lett.*, vol. 103, no. 18, pp. 181122-1–181122-4, Nov. 2013.

[13] A. Žukauskas, V. Melissinaki, D. Kaškelyte, M. Farsari, and M. Malinauskas, "Improvement of the fabrication accuracy of fiber tip microoptical components via mode field expansion," *J. Laser Micro Nanoeng.*, vol. 9, no. 1, pp. 68–72, Feb. 2014.

[14] A. Žukauskas *et al.*, "Black silicon: Substrate for laser 3D micro/nanopolymerization," *Opt. Exp.*, vol. 21, no. 6, pp. 6901–6909, Mar. 2013.

[15] M. Malinauskas *et al.*, "3D microoptical elements formed in a photostructurable germanium silicate by direct laser writing," *Opt. Lasers Eng.*, vol. 50, no. 12, pp. 1785–1788, Dec. 2012.

[16] Y.-L. Sun *et al.*, "Protein-based soft micro-optics fabricated by femtosecond laser direct writing," *Light, Sci. Appl.*, vol. 3, p. e192, Sep. 2014.

[17] S. Kawata, H.-B. Sun, T. Tanaka, and K. Takada, "Finer features for functional microdevices," *Nature*, vol. 412, pp. 697–698, Aug. 2001.

[18] Y.-L. Zhang, Q.-D. Chen, H. Xia, and H.-B. Sun, "Designable 3D nanofabrication by femtosecond laser direct writing," *Nano Today*, vol. 5, no. 5, pp. 435–448, Sep. 2010.

[19] D. Wu *et al.*, "Femtosecond laser rapid prototyping of nanoshells and suspending components towards microfluidic devices," *Lab Chip*, vol. 9, pp. 2391–2394, Jun. 2009.

[20] T. Tanaka, H.-B. Sun, and S. Kawata, "Rapid sub-diffraction-limit laser micro/nanoprocessing in a threshold material system," *Appl. Phys. Lett.*, vol. 80, no. 2, pp. 312–314, Oct. 2002.

[21] Y.-L. Sun *et al.*, "Dynamically tunable protein microlenses," *Angew. Chem. Int. Ed.*, vol. 51, no. 7, pp. 1558–1562, Feb. 2012.

[22] J. L. Liu, Y. Li, M. Chen, and J. Guo, "Numerical calculation of the use of a concave–convex lens for shaping axisymmetric laser beams," *Opt. Laser Technol.*, vol. 40, no. 7, pp. 946–952, Oct. 2008.

[23] D. Wu, J. Xu, L.-G. Niu, S.-Z. Wu, K. Midorikawa, and K. Sugioka, "In-channel integration of designable microoptical devices using flat scaffold-supported femtosecond-laser microfabrication for coupling-free optofluidic cell counting," *Light, Sci. Appl.*, vol. 4, p. e228, Jan. 2015.